Stanford Exploration Project, Report 111, June 10, 2002, pages 17–47

Least-squares joint imaging of primaries and multiples

Morgan Brown[1]

ABSTRACT

Multiple reflections provide redundant, and sometimes additional, information about the corresponding primary reflections. I implement a least-squares inversion scheme to jointly image (by normal moveout) primaries and multiples, with the goal of enforcing consistency between the images and the input data. Furthermore, to effect noise ("crosstalk") suppression, I introduce a novel form of model regularization which exploits kinematic similarities between imaged primaries and multiples, and which also preserves the amplitude-versus-offset (AVO) response of the data. In tests on synthetic data, my approach exhibits good noise suppression and signal preservation characteristics. Real data tests highlight the need for careful data preprocessing. Future work points toward use of migration as the imaging operators, to exploit cases where multiples actually exhibit better angular coverage than primaries, and thus add new information to the inversion.

INTRODUCTION

Multiple reflections have long been treated as noise in the seismic imaging process. In contrast to many other types of "noise", like surface waves, multiply reflected body waves may still penetrate deep into the earth, and thus have a potential to aid in imaging the prospect zone. I refer generically to *joint imaging with multiples* as any process which creates a "pseudo-primary" image from multiples by removing the propogation effects of body waves through arbitrary multiple layer (generator + free surface), and which then seeks to integrate the information provided by the primary and pseudo-primary images.

Reiter et al. (1991) present an early example of imaging multiples directly using a prestack Kirchhoff scheme. Yu and Schuster (2001) describe a cross-correlation method for imaging multiples. Berkhout and Verschuur (1994) and Guitton (2002) apply shot-profile migration for multiples. The aforementioned approaches produce separate-but-complementary pseudo-primary and primary images, yet they either do not attempt to, or employ simplistic methods to integrate the information contained in the two images; either add (Reiter et al., 1991) or multiply (Yu and Schuster, 2001) them together.

In this paper, I introduce a new methodology for jointly imaging primaries and multiples. In addition to a desire to correctly image the multiples, my approach is driven by three primary motivations:

[1]**email:** morgan@sep.stanford.edu

1. **Data Consistency -** The primary and pseudo-primary images both should be maximally consistent with the input data.
2. **Self-consistency** - The primary and pseudo-primary images should be consistent with one another, both kinematically and in terms of amplitudes.
3. **Noise Suppression -** In the primary image, all orders of multiples should be suppressed. In the pseudo-primary image created from, say first-order water-bottom multiples, contributions from primaries and secord-order or greater multiples should be suppressed.

Least squares optimization provides an excellent, and perhaps the only viable approach to address all three requirements. I adopt an approach similar to Nemeth et al. (1999), which used a least-squares scheme to jointly image compressional and surface waves, for improved wavefield separation. Data consistency is effected by minimization of a data residual; self-consistency and noise suppression through the use of regularization terms which penalize 1) differences between primary and pseudo-primary images, and 2) attributes which are not characteristic to true primaries or pseudo-primaries.

In my approach, I use the simplest possible imaging operation, Normal Moveout (NMO). I derive an NMO equation for water-bottom multiple reflections, which maps these multiples to the same zero-offset traveltime as their associated primaries, creating a "pseudo-primary" section. To account for the amplitude differences between the primary and pseudo-primary sections, I assume constant seafloor AVO behavior and estimate a single water-bottom reflection coefficient from the data. To address the AVO differences between primary and pseudo-primary, I derive an expression – valid only for constant velocity – for the AVO of the pseudo-primary as a function of the AVO of the primary, and then enforce this constraint in the inversion via an offset- and time-dependent regularization term.

METHODOLOGY

NMO for Multiple Reflections

In a horizontally-stratified, $v(z)$ medium, multiple reflections can be treated as kinematically-equivalent primaries with the same source-receiver spacing but additional zero-offset traveltime τ^*, as illustrated in Figure 1. We can write an extension to the NMO equation which flattens multiples to the zero-offset traveltime of the reflector of interest.

$$t^2 = \sqrt{(\tau + j\tau^*)^2 + \frac{x^2}{V_{eff}^2}} \tag{1}$$

$j\tau^*$ is the two-way traveltime of a j^{th}-order multiple in the top layer. $V_{eff}(\tau)$ is the effective RMS velocity of the equivalent primary shown in the figure. For the simple case of constant velocity v^* in the multiple-generating layer,

$$V_{eff}(\tau) = \frac{\tau^* v^* + \tau V(\tau)}{\tau^* + \tau} \tag{2}$$

So for the common case of relatively flat reflectors, $v(z)$, and short offsets, equation (1) should do a reasonable job of flattening water-bottom multiples of any order to the τ of interest, assuming that we pick the water bottom (τ^*) and that we know the seismic velocity of water.

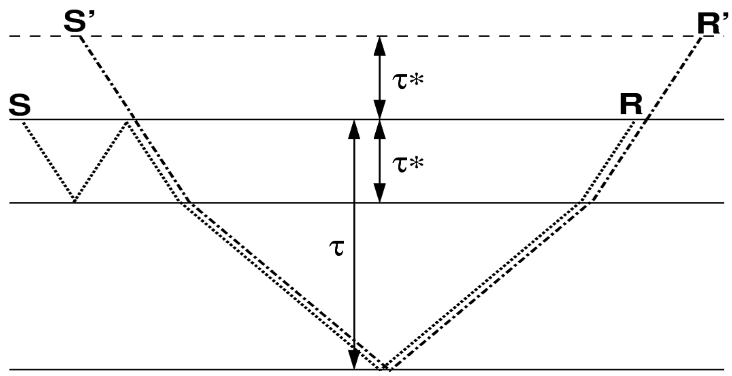

Figure 1: Schematic for NMO of multiples. From the standpoint of NMO, multiples can be treated as pseudo-primaries with the same source-receiver spacing, but with extra zero-offset traveltime τ^*, assuming that the velocity and time-thickness of the multiple layer are known. morgan1-schem [NR]

AVO of Multiple Reflections

Even after application of the water-bottom reflection coefficient, the AVO response of the pseudo-primary section created by equation (1) does not match that of the corresponding NMO-corrected primary section. Refer to Figure 2 and note that for constant-AVO water-bottom reflection (and a free surface reflection coefficient of -1), the amplitude of the water-bottom multiple at offset $h_p + h_m$ is simply the amplitude of the primary at offset h_p, scaled by the negative water-bottom reflection coefficient. Still, the question remains: *what are h_m and h_p?* For the case of constant velocity, we can use trigonometry to derive h_m and h_p as a function of the zero offset traveltimes of the primary reflection and water bottom (τ and τ^*, respectively), and the source-receiver offset x. In constant velocity, the multiple and primary legs of the raypath are similar triangles:

$$\frac{\tau v}{h_p} = \frac{\tau^* v}{h_m}. \tag{3}$$

Also, for a first-order water-bottom multiple,

$$h_p + h_m = x.$$

These two independent equations can be solved and simplified to give expressions for h_p and h_m:

$$h_p = \frac{\tau}{\tau + \tau^*} x \quad \text{and} \quad h_m = \frac{\tau^*}{\tau + \tau^*} x. \tag{4}$$

I omit the general form of the expression for orders of multiple higher than one, although it is straightforward to derive.

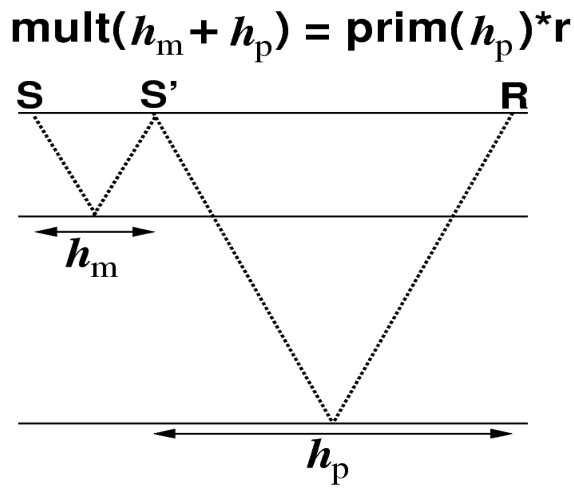

Figure 2: Assuming a constant AVO water-bottom reflection and constant velocity, we can write the AVO of water-bottom multiples with offset $h_p + h_m$ as a function of the AVO of the primary recorded at a shorter offset, h_p. morgan1-avo [NR]

To obtain an estimate of the water-bottom reflection coefficient, I solve a simple least squares problem to estimate a function of location, $\mathbf{a}(x)$, which when applied to a small window of dimension $nt \times nx$ around the NMO-corrected water-bottom reflection, $\mathbf{p}(t,x)$, optimally resembles the NMO-corrected [equation (1)] first-order water-bottom multiple reflection, $\mathbf{m}(t,x)$. To achieve this, $\mathbf{a}(x)$ is perturbed to minimize the following quadratic functional.

$$\min \left(\sum_{j=1}^{nx} \sum_{i=1}^{nt} a(j) * p(i,j) - m(i,j) \right)^2 \tag{5}$$

$\mathbf{a}(x)$ may not be reliable at far offsets, due to either NMO stretch or non-hyperbolicity, so in practice, an estimate of the single best-fitting water-bottom reflection coefficient is made using the $\mathbf{a}(x)$ from “useful” offsets only.

Least-squares imaging of multiples

Applied to a common-midpoint gather, equation (1) produces an approximate unstacked zero-offset image of pseudo-primaries from water bottom multiple reflections. In this section, I introduce a least squares scheme to compute self-consistent images of primaries and pseudo-primaries which are in turn consistent with the data. First I define some terms:

$\mathbf{d}$ $\leftrightarrow$ One CMP gather.

$\mathbf{m}_j$ $\leftrightarrow$ Prestack model vector for multiple order j. Produced by applying equation (1) to $\mathbf{d}$.

$\mathbf{N}_j$ $\leftrightarrow$ *Adjoint* of NMO for multiple of order j (primaries: $j=0$). $\mathbf{N}_j^T$ applies equation (1) to $\mathbf{d}$.

$\mathbf{R}_j$ $\leftrightarrow$ Given a single water-bottom reflection coefficient, r, [estimated via equation (5)], this operator scales $\mathbf{m}_j$ by $1/r^j$ to make the amplitudes of all the $\mathbf{m}_j$ comparable.

With these definitions in hand, we can now write the forward modeling operator for joint NMO of primaries and multiples of order 1 to p.

$$\begin{bmatrix} \mathbf{N}_0 & \mathbf{N}_1\mathbf{R}_1 & \cdots & \mathbf{N}_p\mathbf{R}_p \end{bmatrix} \begin{bmatrix} \mathbf{m}_0 \\ \mathbf{m}_1 \\ \vdots \\ \mathbf{m}_p \end{bmatrix} = \mathbf{L}\mathbf{m} \tag{6}$$

In words, equation (6) takes a collection of psuedo-primary panels, divides each by the appropriate reflection coefficient, applies inverse (adjoint) NMO to each, and then sums them together to create something that should resemble “data”. We define the data residual as the difference between the input data and the forward-modeled data:

$$\mathbf{r}_d = \mathbf{d} - \mathbf{L}\mathbf{m} \tag{7}$$

Viewed as a standard least-squares inversion problem, minimization of L_2 norm of the data residual by solution of the normal equations is underdetermined. Additional regularization terms, defined in later sections, force the problem to be overdetermined.

Consistency of the Data and the Crosstalk Problem

Figure 3 shows the result of applying the adjoint of equation (6) to a synthetic CMP gather which was constructed by an elastic modeling scheme. Imagine for a moment that the CMP gather consists *only* of primaries and first- and second-order water-bottom multiples. The “NMO for Primaries” panel would contain flattened primaries (signal) and downward-curving first- and second-order multiples (noise). Likewise, the “NMO for multiple 1” and “NMO for multiple 2” panels contain flattened signal and curving noise. Why do I call these components “signal” and “noise”? If each of the three panels contained all signal and no noise, then we could 1) perfectly reconstruct the data from the model by applying equation (6), and 2) be in the enviable position of having a perfect estimate of the primaries.

Unfortunately, the curved events – so-called “crosstalk” – in all three model panels spoil this idealized situation (Claerbout, 1992). Because the crosstalk events map back to actual events in the data, they are difficult to suppress in a least-squares minimization of the data residual [equation (7)]. Nemeth et al. (1999) shows that crosstalk relates directly to non-invertibility of the Hessian ($\mathbf{L}^T\mathbf{L}$), and that data-space or model-space regularization may partially overcome the difficulty. In the following section, I introduce a novel form of model-space regularization which promotes discrimination of signal from crosstalk.

Regularization of the Least-Squares Problem

Visual inspection of Figure 3 motivates the two forms of regularization utilized in this paper. Find any first-order multiple on the section marked “NMO for Primaries”. Notice that the corresponding event on the first- and second-order pseudo-primary panels, originally second-

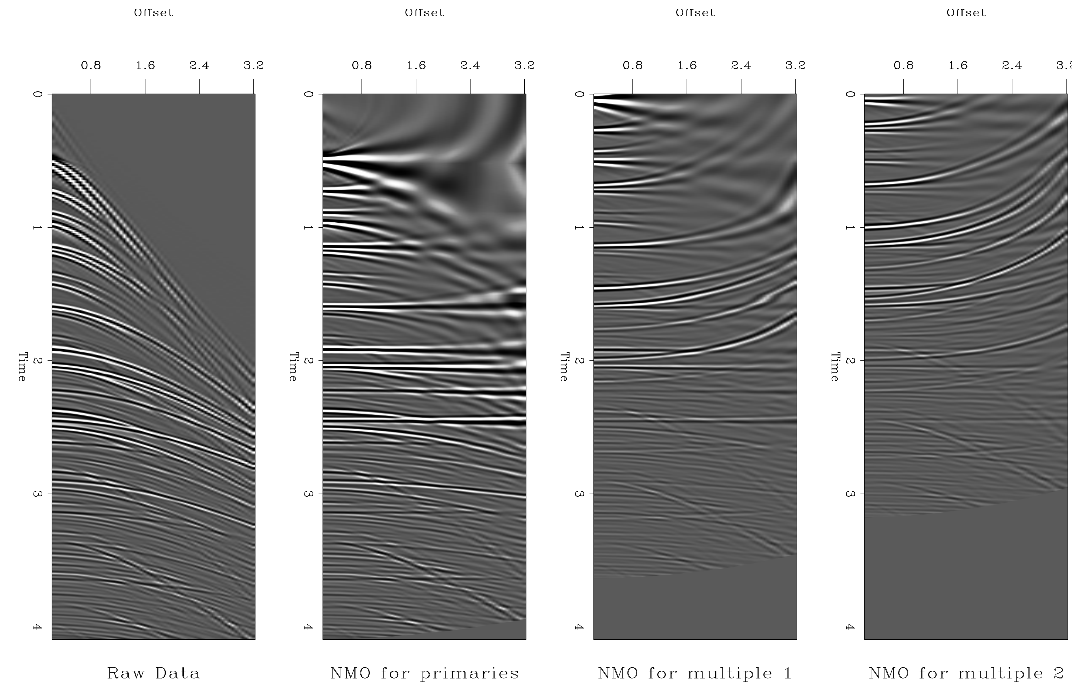

Figure 3: From left to right: Raw synthetic CMP gather; Conventional NMO applied to data; NMO for first-order water-bottom multiple; NMO for second-order water-bottom multiples. morgan1-schem.hask [ER]

and third-order multiples, respectively, all have a different moveout. In fact, the only events which are kinematically consistent across all offsets are the flattened primary and pseudo-primaries. The other events, all crosstalk, are inconsistent between panels. Therefore, the first regularization operator seeks to penalize the difference between the $\mathbf{m}_i$, at fixed τ. To account for the dissimilarity of the AVO of primaries and multiples, this difference is taken at different offsets, as defined in equation (4). Written in the form of a model residual vector, this difference is:

$$\mathbf{r}_m^{[1]}(\tau, x, i) = m_i(\tau, h_p) - m_{i+1}(\tau, x). \tag{8}$$

The third index in equation (9), i, ranges from 0 to $n_p - 1$, where n_p is the highest order multiple modeled in the inversion [see equation (6)].

The second form of regularization used in this paper is the more obvious of the two: a difference operator along offset. This difference exploits the fact that all non-primaries are not flat after NMO. Again, we can write this difference in the form of a model residual vector:

$$\mathbf{r}_m^{[2]}(\tau, x, i) = m_i(\tau, x) - m_i(\tau, x + \Delta x). \tag{9}$$

The second regularization is applied to all the $\mathbf{m}_i$. A similar approach is used by Prucha et al. (2001) to regularize prestack depth migration in the angle domain.

Combined Data and Model Residuals

To compute the optimal set of $\mathbf{m}_i$, a quadratic objective function, $Q(\mathbf{m})$, consisting of sum of the weighted norms of a data residual [equation (7)] and of two model residuals [equations (8) and (9)], is minimized via a conjugate gradient scheme:

$$\min Q(\mathbf{m}) \;=\; \|\mathbf{r}_d\|^2 \;+\; \epsilon_m^2 \|\mathbf{r}_m^{[1]}\|^2 \;+\; \epsilon_x^2 \|\mathbf{r}_m^{[2]}\|^2 \qquad (10)$$

ϵ_m and ϵ_x are scalars which balance the relative weight of the two model residuals with the data residual.

RESULTS

Testing the Raw Algorithm

We begin with the results of testing the proposed algorithm on a single synthetic CMP gather, which was shown previously in Figure 3. This gather, generated using Haskell-Thompson elastic modeling, with earth properties drawn from a well log provided with the “Mobil AVO” dataset (see (Lumley et al., 1994) for a description of data details), has traditionally found use at SEP as a multiple suppression benchmark (Lumley et al., 1994; Nichols, 1994; Clapp and Brown, 1999; Guitton, 2000; Clapp and Brown, 2000). The data contain all surface-related and internal multiples, as well as P-to-S-to-P converted waves.

Figure 4 illustrates the application of the proposed algorithm to the so-called “Haskell” data. Comparing the raw data and the estimated primary panels [$\mathbf{m}_0$ in equation (6)], we see that my algorithm does a decent job of suppressing the strongest multiples, especially at far offsets, though some residual multiple energy remains at the near offsets. We expect poorer performance at near offsets; recall that the first regularization operator [equation (8)] penalizes dissimilarity of events across orders of multiple, yet all orders of multiple align at near offsets. Moreover, the second regularization operator [equation (9)] penalizes residual curvature, yet all events in the section, both primaries and the residual multiples, are flat at near offsets.

The difference panel shows little residual primary energy, which illustrates the favorable signal preservation capability of my approach. The bulk of the residual primary energy exists at far offsets and small times, where NMO stretch makes the primaries nonflat, and hence, vulnerable to smoothing across offset by equation (9).

The bottom three panels in Figure 4 show the data residual [equation (7)], and the first two panels of the two model residuals [equations (9) and (8), respectively]. Put simply, the data residual consists of events which are not modeled by equation (6) – hopefully, the multiples only. The model residuals consist roughly of the portions of the model which were removed by the two regularization terms (again, hopefully multiples only): high-wavenumber events and events which are inconsistent from one panel to the next.

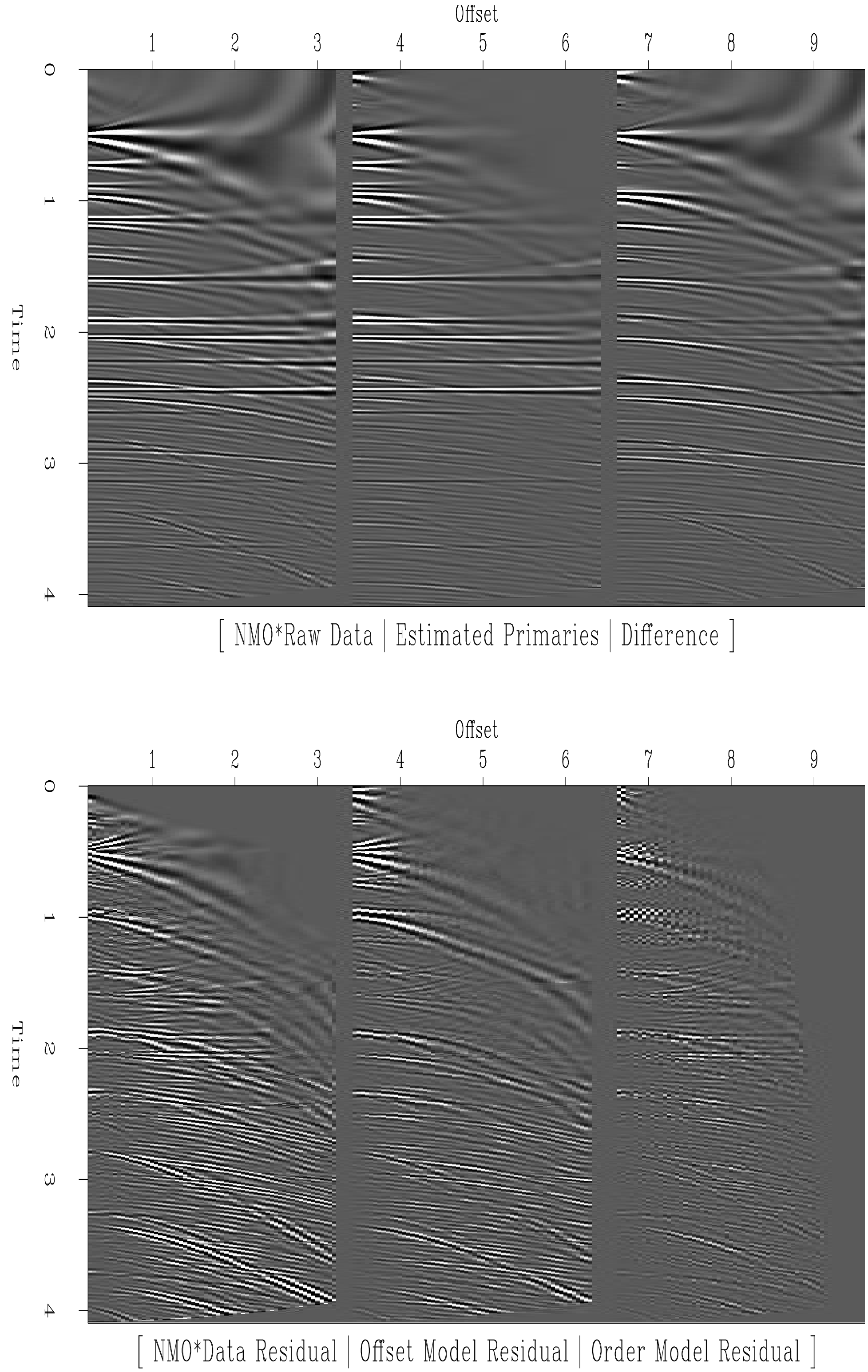

Figure 4: Test of equation (10) on Haskell synthetic CMP gather. Top row, left to right: Raw Haskell data, NMO applied; Estimated primary panel; difference panel. Bottom row, left to right: Data residual; first panel of model residuals, equations (9) and (8), respectively. morgan1-cmps.lsrow.hask [ER]

Better Understanding the Regularization

Figure 5 illustrates the effect of setting $\epsilon_x = 0$ in equation (10), which removes the influence of the regularization term which roughens the model across offset [equation (9)]. The results are intriguing. Most noticeably, leftover multiple reflections in the "Estimated Primaries" panel appear to be scrambled over offset, while primaries appear mostly intact. Signal-to-noise ratio has increased considerably. The fact that the roughener across offset decorrelates the residual multiples should be further exploited.

Notice that the model residual is zero at long offsets and small times. This is due to the fact that the difference is not taken across the same offsets, to account for the AVO multiples, according to equation (4). When $h_p + h_m > h_{max}$, no difference is taken.

Devil's Advocate: What do the Multiples Add?

Figure 6 illustrates application of the algorithm without the use of multiples. Only the regularization across offset, equation (9), is in operation. Though we see some suppression of multiples, the results are not nearly as good as those in Figure 4. More insidiously, note the presence of considerable of primary energy in the difference panel. When exploited as a constraint against crosstalk, the multiple reflections add considerable information. My approach integrates this information in a systematic framework.

A Real Data Example

I test the proposed algorithm on a single CMP gather from the Mobil AVO dataset, described above. The results are shown in Figure 7. Relative to the results seen on the Haskell synthetic, they are fairly poor. On the bright side, notice decent preservation of signal amplitude. The earliest water-bottom multiples are suppressed quite effectively, although the later reverberations are left almost untouched.

The reasons for the less-than-perfect are likely numerous. First, and most important, the multiple reflections quickly become incoherent with an increasing number of bounces. They match well with the primaries only for the strongest reflections. I estimated a relatively small water-bottom reflection coefficient, 0.1, so the multiples are relatively weak in amplitude. I did not perform any preprocessing on the data, and I believe they were donated to SEP as raw gathers. Berlioux and Lumley (1994) applied cable balancing to the Mobil AVO dataset. High-wavenumber, offset-variant amplitude variations along events spoil the ability regularization equation (8) to discriminate against crosstalk.

DISCUSSION

I presented a new approach for the joint imaging of primary and multiple reflections. My approach goes further than the separate imaging of multiples and primaries. I integrate infor-

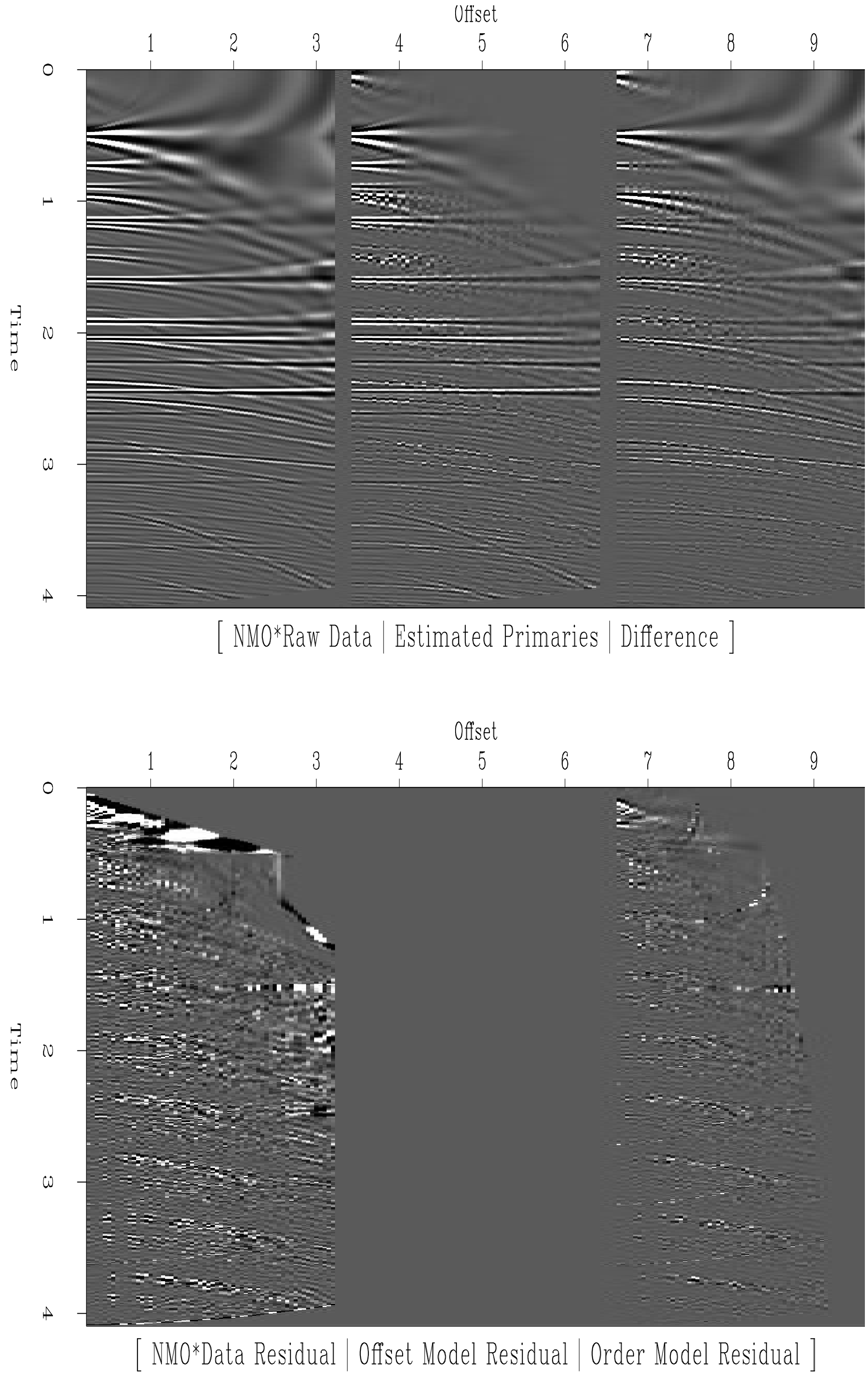

Figure 5: Only the regularization which roughens across orders of pseudo-primary, equation (8), is used in the inversion. Top row, left to right: Raw Haskell data, NMO applied; Estimated primary panel; difference panel. Bottom row, left to right: Data residual; first panel of model residuals, equations (9) and (8), respectively. morgan1-cmps.nograd.hask [ER]

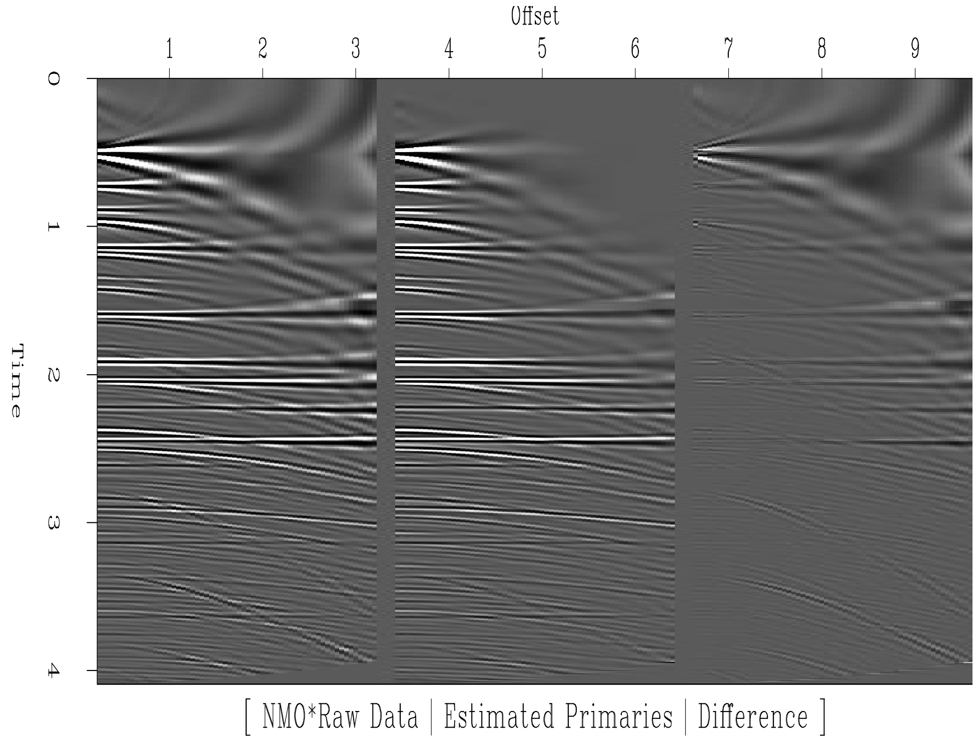

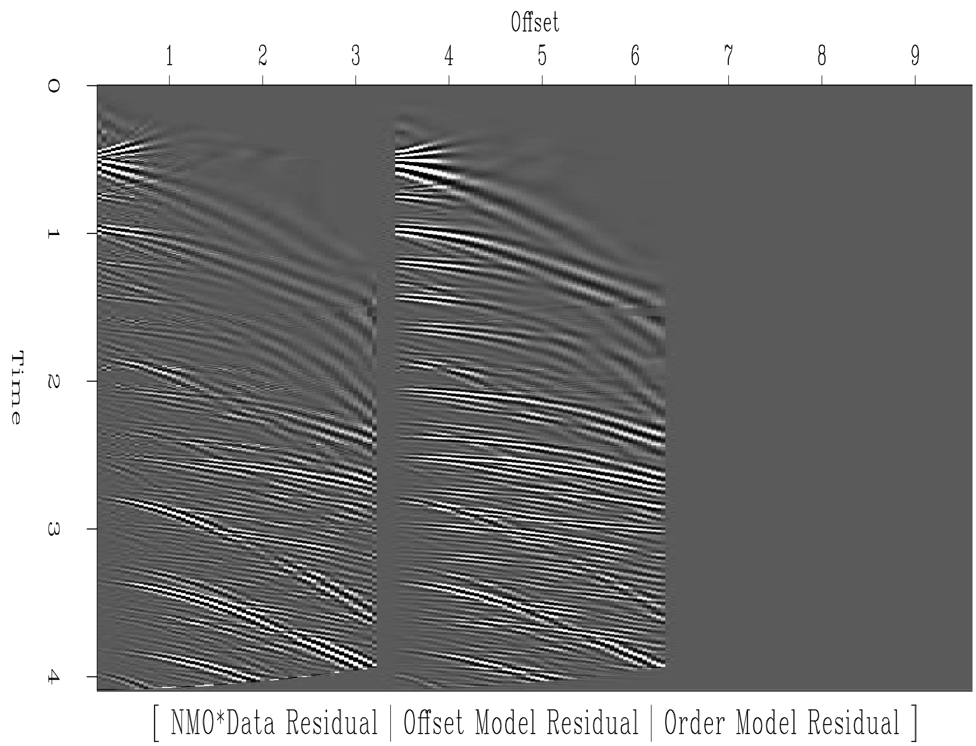

Figure 6: Only the regularization which roughens across offset, equation (9) is used in the inversion. Only one order of pseudo-primary is used, so no information is added by the multiples. Top row, left to right: Raw Haskell data, NMO applied; Estimated primary panel; difference panel. Bottom row, left to right: Data residual; first panel of model residuals, equations (9) and (8), respectively. morgan1-cmps.devils.hask [ER]

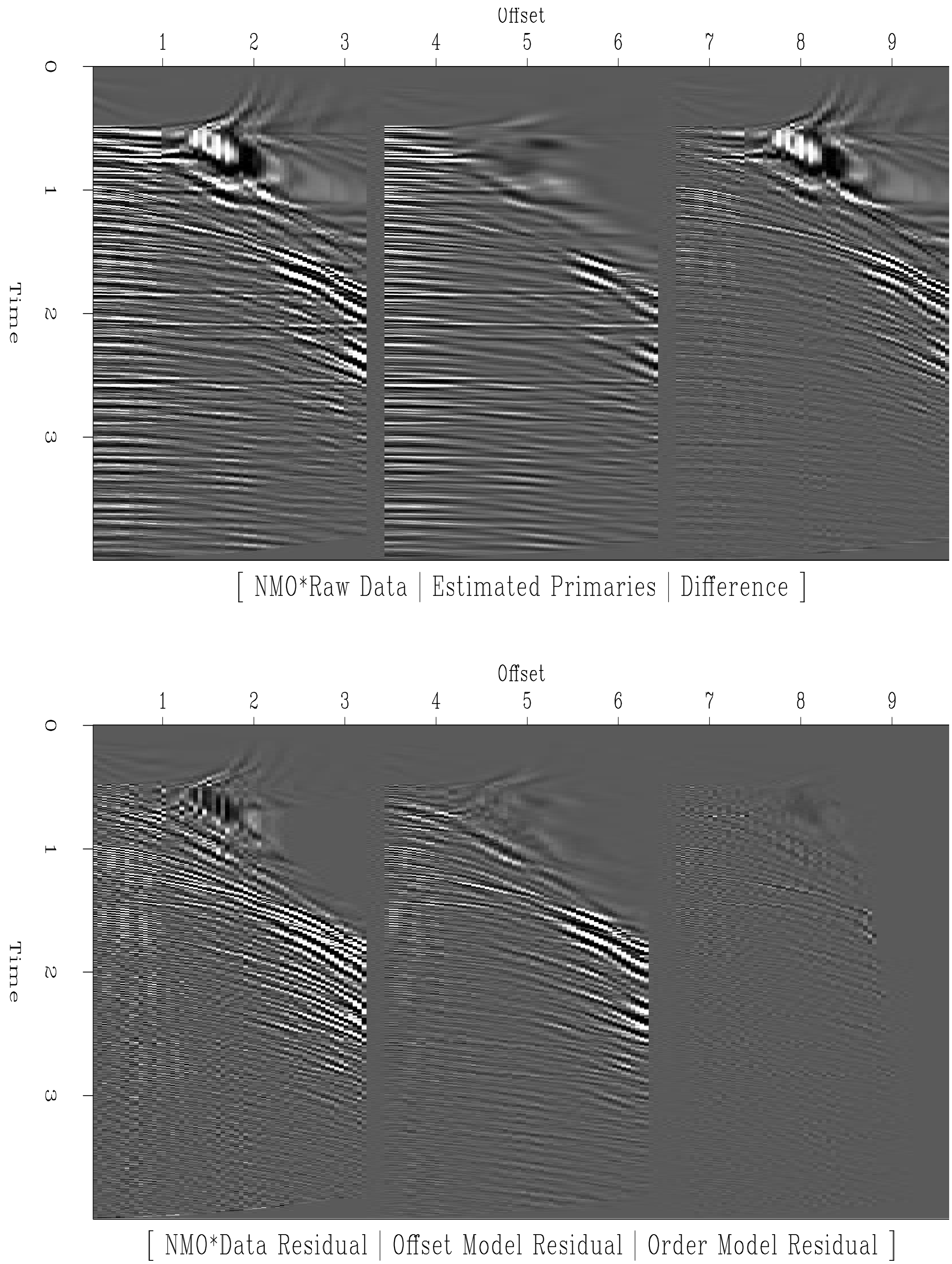

Figure 7: Application of equation (10) to CMP from Mobil AVO data. Top row, left to right: Raw CMP gather, NMO applied; Estimated primary panel; difference panel. morgan1-cmps.lsrow.haskreal [ER]

mation from the multiples and primaries in a least-squares inversion, via a new regularization term which exploits the kinematic similarity of primaries and pseudo-primaries, and the kinematic dissimilarity of crosstalk terms to obtain a noise-free image of the primaries.

The proposed algorithm demonstrates good noise suppression and signal preservation characteristics in the synthetic tests of Figure 4. Comparison of Figures 5 and 6 proves the validity of the new regularization term, equation (8), and more importantly, that the multiples provide valuable information in the inversion.

The results of testing a real data gather were mixed. I believe the single largest problem in this case is poor coherency of the water-bottom multiples. As the water bottom and most shallow reflectors on the Mobil AVO dataset are nearly perfectly flat, geologic complexity is surely not to blame. More likely, the solution(s) to the trouble is(are) more mundane; things like source/cable balancing and spherical divergence. An accurate RMS velocity function is important to success, but errors can be tolerated. Velocity errors lead to curvature in NMO'ed primaries and pseudo-primaries, but as I have dealt here only with water-layer multiples, the real danger, a large phase shift between primaries and pseudo-primaries, is somewhat unlikely.

In all tests, the removal of multiples at near offsets was incomplete. Since the near offsets contribute most to residual multiple energy in the stack, it is of crucial importance to improve performance.

FUTURE DIRECTIONS

The obvious direction in which to move this project is migration. By using migration, rather than NMO, as the imaging operator, the limiting assumptions of NMO ($v(z)$, flat reflectors) can be abandoned. Furthermore, the limitations of operating in the offset domain can be overcome by moving to the more intuitive angle domain. In some cases, multiples provide better angular coverage over a recorded cable length. Systematic integration of this extra information could prove revolutionary in regions of poor illumination. But the fruits of this transition are not without challenges. Because NMO is a vertical mapping, each CMP can be processed independently, making the memory requirements of the current implementation reasonable, and parallelization quite simple. Correctly handling the transformation of amplitudes between primary and pseudo-primary may prove even more of a challenge. Also, regardless of whether NMO or migration is used, the move to 3-D is never a forgiving one from the computational standpoint.

ACKNOWLEDGEMENT

Thanks go to ExxonMobil for providing SEP with the Mobil AVO dataset.

REFERENCES

Berkhout, A. J., and Verschuur, D. J., 1994, Multiple technology: Part 2, migration of multiple reflections: 64th Ann. Internat. Mtg, Soc. Expl. Geophys., Expanded Abstracts, 1497–1500.

Berlioux, A., and Lumley, D., 1994, Amplitude balancing for AVO analysis: SEP–**80**, 349–360.

Claerbout, J. F., 1992, Earth Soundings Analysis: Processing Versus Inversion: Blackwell Scientific Publications.

Clapp, R. G., and Brown, M., 1999, Applying sep's latest tricks to the multiple suppression problem: SEP–**102**, 91–100.

Clapp, R. G., and Brown, M., 2000, $(t-x)$ domain, pattern-based multiple separation: SEP–**103**, 201–210.

Guitton, A., 2000, Prestack multiple attenuation using the hyperbolic Radon transform: SEP–**103**, 181–201.

Guitton, A., 2002, Shot-profile migration of multiple reflections: SEP–**111**, 17–33.

Lumley, D., Nichols, D., and Rekdal, T., 1994, Amplitude-preserved multiple suppression: SEP–**82**, 25–45.

Nemeth, T., Wu, C., and Schuster, G. T., 1999, Least-squares migration of incomplete reflection data: Geophysics, **64**, no. 1, 208–221.

Nichols, D., 1994, Velocity-stack inversion using $\mathbf{L_p}$ norms: SEP–**82**, 1–16.

Prucha, M. L., Clapp, R. G., and Biondi, B. L., 2001, Imaging under salt edges: A regularized least-squares inversion scheme: SEP–**108**, 91–104.

Reiter, E. C., Toksoz, M. N., Keho, T. H., and Purdy, G. M., 1991, Imaging with deep-water multiples: Geophysics, **56**, no. 07, 1081–1086.

Yu, J., and Schuster, G., 2001, Crosscorrelogram migration of IVSPWD data: 71st Ann. Internat. Mtg, Soc. Expl. Geophys., Expanded Abstracts, 456–459.